

University of Groningen

**Microstructural and frictional control of diamond-like carbon films deposited on acrylic rubber by plasma assisted chemical vapor deposition**

Martinez-Martinez, D.; Schenkel, M.; Pei, Y.T.; Hosson, J.Th.M. De

*Published in:*  
Thin Solid Films

*DOI:*  
[10.1016/j.tsf.2010.11.006](https://doi.org/10.1016/j.tsf.2010.11.006)

**IMPORTANT NOTE: You are advised to consult the publisher's version (publisher's PDF) if you wish to cite from it. Please check the document version below.**

*Document Version*  
Publisher's PDF, also known as Version of record

*Publication date:*  
2011

[Link to publication in University of Groningen/UMCG research database](#)

*Citation for published version (APA):*

Martinez-Martinez, D., Schenkel, M., Pei, Y. T., & Hosson, J. T. M. D. (2011). Microstructural and frictional control of diamond-like carbon films deposited on acrylic rubber by plasma assisted chemical vapor deposition. *Thin Solid Films*, 519(7), 2213-2217. <https://doi.org/10.1016/j.tsf.2010.11.006>

**Copyright**

Other than for strictly personal use, it is not permitted to download or to forward/distribute the text or part of it without the consent of the author(s) and/or copyright holder(s), unless the work is under an open content license (like Creative Commons).

The publication may also be distributed here under the terms of Article 25fa of the Dutch Copyright Act, indicated by the "Taverne" license. More information can be found on the University of Groningen website: <https://www.rug.nl/library/open-access/self-archiving-pure/taverne-amendment>.

**Take-down policy**

If you believe that this document breaches copyright please contact us providing details, and we will remove access to the work immediately and investigate your claim.

Downloaded from the University of Groningen/UMCG research database (Pure): <http://www.rug.nl/research/portal>. For technical reasons the number of authors shown on this cover page is limited to 10 maximum.



# Microstructural and frictional control of diamond-like carbon films deposited on acrylic rubber by plasma assisted chemical vapor deposition

D. Martinez-Martinez<sup>\*</sup>, M. Schenkel, Y.T. Pei, J.Th.M. De Hosson

Department of Applied Physics, Materials Innovation Institute M2i, University of Groningen, Nijenborgh 4, 9747 AG Groningen, The Netherlands

## ARTICLE INFO

### Article history:

Received 27 August 2010

Accepted 2 November 2010

Available online 10 November 2010

### Keywords:

Scanning electron microscopy

Plasma assisted chemical vapor deposition

Rubber

Coefficient of friction

## ABSTRACT

In this paper we concentrate on the microstructure of diamond-like carbon films prepared by plasma assisted chemical vapor deposition on acrylic rubber. The temperature variation produced by the ion impingement during plasma cleaning and subsequent film deposition was monitored and controlled as a function of bias voltage and treatment time. Its influence during film growth on the appearance of patterns of cracks and wrinkles, caused by the thermal stresses is evaluated. Different growth modes are proposed in order to explain the smaller patch sizes observed at negative variations of temperature. The coefficient of friction (CoF) of the samples is measured using a pin-on-disk tribometer in non-lubricated conditions. Much lower CoF values than unprotected rubber are seen, which can be correlated with the observed patch size.

© 2010 Elsevier B.V. All rights reserved.

## 1. Introduction

Ball bearings are used in many technical fields, like aerospace or automotive industries [1]. In many cases, a rubber seal is incorporated in order to prevent the leakage of lubricant and the entrance of dirt. However, under these conditions, dynamic rubber seals suffer from severe wear and cause high friction, leading to an ultimate failure of the bearing. Diamond-like carbon (DLC) films are optimal solutions as protective coatings, due to the combination of relatively high hardness, chemical inertness, low friction coefficient and low wear rates [2]. Further requirements are film flexibility and an excellent adhesion to the rubber substrate. The chemical nature of the rubber, which is mainly composed by C and H, suggests a good compatibility with a carbonaceous film.

The deposition of these kinds of films on rubber has been reported previously [3], where a grid is used to produce a tile-like film for maintaining flexibility. The presence of this grid led to unprotected areas on the substrate, which caused deterioration of the film, and as a consequence the coefficients of friction (CoF) were still rather high (around 1).

The aim of this work is to study the influence of process parameters (namely, bias voltage and temperature change during film growth) on the microstructure and CoF of DLC films deposited on acrylic rubber (ACM) by plasma assisted chemical vapor deposition (PACVD). The formation of self-patterned structures with good flexibility, adhesion to rubber and low CoF are investigated.

## 2. Experimental details

### 2.1. Process description and temperature measurement

Carbonaceous thin films were deposited on acrylic rubber (alkyl acrylate copolymer, ACM) by means of PACVD in a Teer UDP/400 close field unbalanced magnetron sputtering rig, with all the magnetrons powered off. A pulsed DC (p-DC) power unit (Advanced Energy) was used as substrate bias source, operating at 250 kHz with a pulse off time of 500 ns and voltages between 300 and 600 V. Four pieces of ACM rubber (50×50×2 mm) were coated in each batch. Before deposition, the rubber substrates were cleaned by two subsequent wash procedures, in order to improve the film adhesion by removal of the dirt and the wax present in the rubber, respectively [4]. The first treatment comprised of five cycles of ultrasonic washing in a 10 vol.% solution of detergent (Superdecontamine 33 from N.V. Intersciences S.A., Brussels) in demineralized water at 60 °C for 15 min each cycle. The second one corresponded to five cycles of ultrasonic washing in boiling demineralized water for 15 min each cycle.

The deposition process was composed of three steps. At the first one, the ACM samples were etched for 30–40 min in an Ar plasma (15 sccm,  $5 \times 10^{-3}$  mbar), in order to further clean the surface from contaminations. Then, a second treatment in a plasma mixture of Ar and H<sub>2</sub> (flow ratio 15:10 sccm,  $6 \times 10^{-3}$  mbar) was used in order to improve the adhesion of the forthcoming carbonaceous layer. These two steps are labeled as ‘etching’ steps, in contrast to the final one where H<sub>2</sub> is replaced by C<sub>2</sub>H<sub>2</sub> (10 sccm) and then DLC film was deposited. However, the residual hydrogen in the inlet pipeline used also for acetylene might last till the first 10 min of deposition, during which the growth of DLC film is only minor.

<sup>\*</sup> Corresponding author.

E-mail address: [d.martinez-martinez@m2i.nl](mailto:d.martinez-martinez@m2i.nl) (D. Martinez-Martinez).

During the etching and deposition processes, the temperature of the rubber varied as an effect of the impinging ions. In order to measure the temperature variations during that process, a type K thermocouple (ungrounded junction, with compacted MgO as electrical isolator surrounded by a metallic sheath) was inserted into an ACM rubber sheet (see Fig. 1). The temperature could be continuously recorded without interruption of the plasma, since it did not affect the readings of the thermocouple in absence of direct contact with the conductive sample holder. In order to fit the data, the plasma was considered as a 'hot body', whose temperature is constant ( $T_{eq}$ ). Then, the heat flow from plasma to the substrate ( $Q$ ) would be governed by Fourier's law:

$$\frac{\partial Q}{\partial t} = -\lambda A \frac{\partial T}{\partial x} \quad (1)$$

where  $t$  is the time,  $T$  is the temperature,  $x$  represents the distance to the substrate,  $A$  is the substrate area, and  $\lambda$  is the thermal conductivity. The temperature variation for a given heat transfer is controlled by the specific heat capacity ( $c$ ) and the mass ( $m$ ):

$$\Delta T = \frac{Q}{c \cdot m} \quad (2)$$

Eqs. (1) and (2) can be combined to reach the following expression:

$$\frac{dT}{dt} = -K \cdot \Delta T = -K \cdot (T - T_{eq}) \quad (3)$$

where  $K^{-1}$  can be defined as the time needed for reaching the temperature  $T(K^{-1}) = T_{eq} - \left(\frac{T_{eq} - T_0}{e}\right)$ . This constant represents the difficulty to increase the temperature of the substrate and depends on materials properties (density, thermal conductivity, heat capacity) and geometry, but it can be considered independent of temperature for small variations:

$$K \propto \frac{\lambda \cdot A}{c \cdot m \cdot x} = \frac{\lambda}{c \cdot \rho \cdot x \cdot \tau}$$

where  $\rho$  and  $\tau$  are the density and thickness of the rubber, respectively.

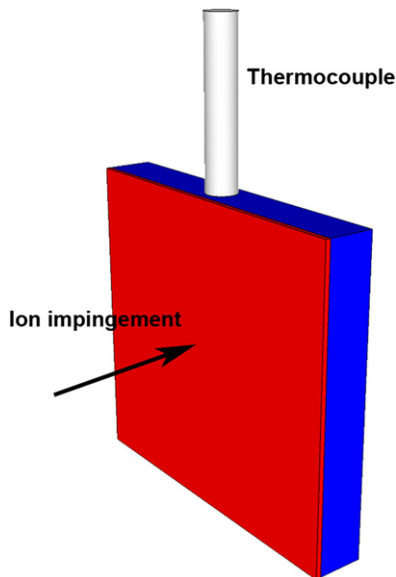


Fig. 1. Scheme of the system used for temperature measurement.

The solution of Eq. (3) is:

$$\ln \left( \frac{T - T_{eq}}{T_0 - T_{eq}} \right) = -Kt \quad (4)$$

The results of temperature measurements and the fittings according to Eq. (4) are displayed in Fig. 2a. It can be observed that the fittings represent the experimental trends very well. Besides, the same value of  $K$  ( $K = 0.056 \text{ min}^{-1}$ ) could be used, indicating that the measurements were properly reproducible. The values of  $T_{eq}$  are found to increase with the applied voltage in a soft parabolic manner, as seen in Fig. 2b. This procedure allowed us to set the plasma treatment by adjusting the bias voltage, in order to obtain different temperature variations during the growth of the film ( $\Delta T$ ). To keep a constant film thickness of  $\sim 300 \text{ nm}$ , the deposition durations were adjusted according to the bias voltage applied.

## 2.2. Sample preparation and characterization

Several deposition protocols were defined in order to study the effect of temperature profiles on the microstructure and frictional performance of different films (see Table 1). These protocols can be divided into *single*, if the voltage during the deposition is kept constant, or *double*, if the voltage is changed during deposition. Therefore, in the former case, only one value of  $\Delta T$  is obtained during deposition, whereas in the latter case two values of  $\Delta T$  are obtained. The films are labeled according to the sign of the temperature variation during film growth. Thus, P, N and Z are used for films deposited using protocols with positive, negative and zero temperature variations, respectively. In the case of double protocols, combinations of the aforementioned labels are used (e.g. PN and NP).

The protocols examined are displayed in Fig. 3. Fig. 3a shows those starting with a bias voltage of 300 V for etching. One of them (sample P) is single, with  $\Delta T = 101^\circ \text{C}$ . The second one (sample PN) is double, and it has a temperature profile similar to the previous one except at the end where a negative  $\Delta T$  is applied by lowering the bias voltage. The temperature variations during this deposition are  $\Delta T = 90^\circ \text{C}$  and  $\Delta T = -80^\circ \text{C}$ , which are shortened as  $\Delta T = 90/-80$ . Fig. 3b shows the protocols starting with a voltage of 600 V. Three of these protocols are single (films Z, N, and N2), although in sample Z two different voltages are used during the etching step in order to reach a constant temperature in a faster manner. The last protocol (sample NP) is double, similar to the one used for sample N, but finished using a 600 V step in order to increase the temperature at the end of the deposition.

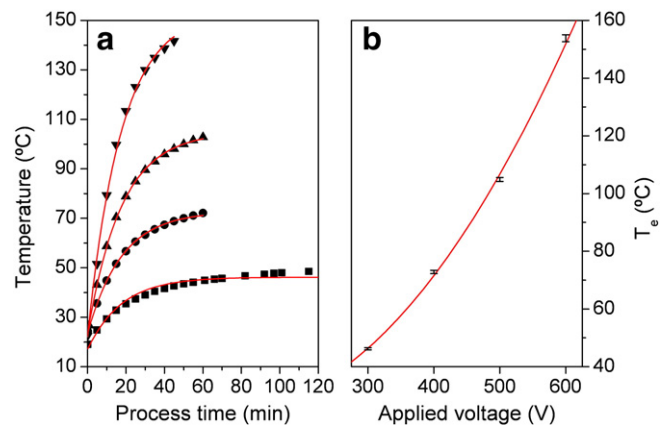
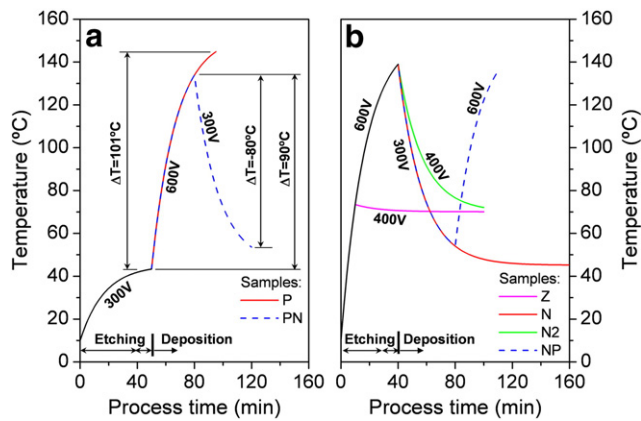


Fig. 2. a) Measured substrate temperature profile at different bias voltages indicated. The lines are the fittings according to Eq. (4). b) Values of  $T_{eq}$  depending of the bias voltage. The line represents a parabolic fitting.

**Table 1**  
Characteristics of DLC films deposited on ACM.

Film code	Etching voltage (time)	Deposition voltage (time)	$\Delta T_1$ (°C)	$\Delta T_2$ (°C)	Patch size ( $\mu\text{m}$ )
P	300 V (50 min)	600 V (45 min)	101	—	124
PN		600 V (30 min) 300 V (40 min)	90	−80	100
Z	600 V (10 min), 400 V (30 min)	400 V (60 min)	0	—	—
N	600 V (40 min)	300 V (120 min)	−94	—	38
N2		400 V (60 min)	−68	—	77
NP		300 V (40 min), 600 V (30 min)	−85	82	80



**Fig. 3.** Temperature-time protocols used in this study as described in Table 1. a) Protocols starting with 300 V plasma etching. The observed values of  $\Delta T$  for both protocols are shown. b) Protocols starting with 600 V plasma etching. Both etching steps (first in Ar and then in Ar/H<sub>2</sub> plasma) and deposition steps are indicated with arrows. The voltages used in each process are also included.

The microstructure was characterized by scanning electron microscopy (SEM), using a Philips FEG-XL30s operating at 3 kV acceleration voltage. Cross sections of DLC film coated ACM were obtained by fracture after immersion in liquid nitrogen for 10 min. The CoF of the films were evaluated in a CSM ball-on-disk system

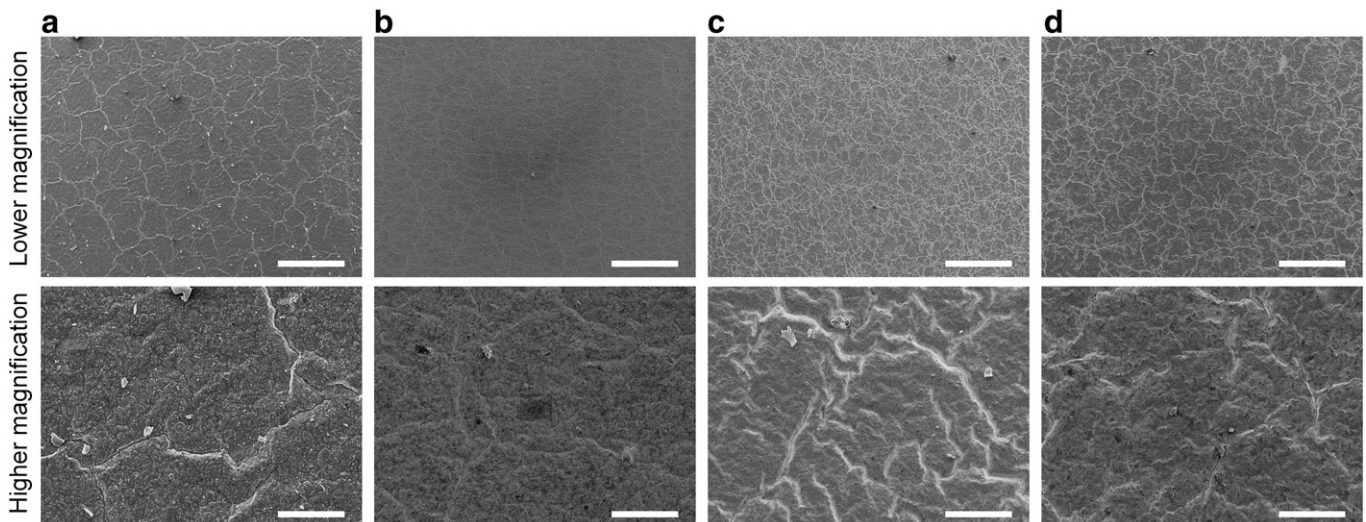
operating in unlubricated sliding against  $\varnothing 6$  mm 100Cr6 steel balls in air at a relative humidity of  $35 \pm 2\%$ . The test parameters were set to 1 N of normal load, 20 cm/s of linear speed, and 10,000 laps of sliding distance.

### 3. Results and discussion

Fig. 4 shows the microstructure of DLC films deposited with single temperature profiles. It can be seen that the film P, prepared while temperature rises, shows a crack pattern with an average patch size of  $124 \mu\text{m}$ . In contrast, the film Z exhibits no cracks, as could be expected considering that the temperature was kept constant during the growth. Fig. 4c and d shows two films prepared under a negative temperature variation. In both cases, the films are characterized by a dense network of wrinkles. It can be seen that the film N shows a smaller patch size ( $39 \mu\text{m}$ ) than the film N2 ( $77 \mu\text{m}$ ), due to a larger compressive deformation occurring in the former case because of the larger variation of temperature. However, it is worth mentioning that the patch size observed in the film N is much smaller than in the film P, although the absolute values of  $\Delta T$  (and hence the deformations) are close.

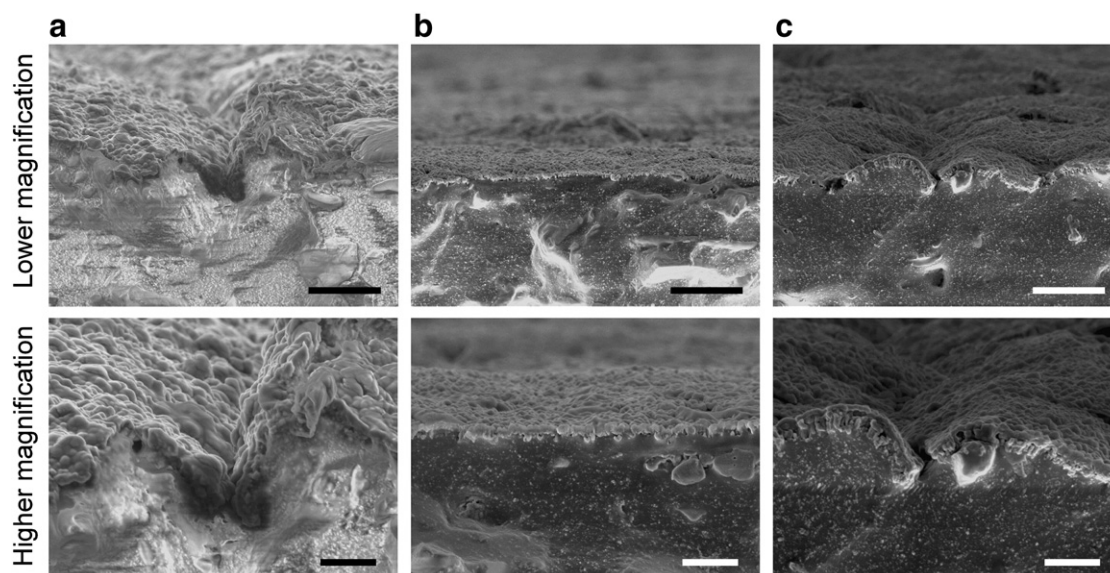
This fact indicates that the mechanisms behind the crack and wrinkle formation are different, and depend on the sign of the temperature variation. In order to get a deeper insight into this phenomenon, cross-section SEM micrographs were taken for those films (P and N), together with the one grown at  $\Delta T = 0$  (film Z) for the sake of comparison (see Fig. 5). In the case of the film P, only one crack appears in the micrograph. The crack is closed, with inward bended edges that touch each other. This effect occurs during the cooling from the temperature at the end of the deposition ( $\sim 145^\circ\text{C}$ ) to room temperature. In contrast, the film Z shows a non-deformed continuous structure and almost flat, in agreement with the top view image. Film N shows a wrinkled structure, with discontinuities at the edge of each patch that are curved (convex outwards). In this case, it can be seen that they do not appear as closed as in the case of film P. In addition, the amount of discontinuities is larger than in the case of film P, as already observed in top view images.

Fig. 6 shows a scheme of the growth of both films with  $\Delta T \neq 0$ . In the case of film P (see Fig. 6a), the substrate expands as the temperature rises. At the beginning of deposition, the growth is columnar, with columns being separated from each other due to the expansion of the rubber substrate. However, the rate of expansion decreases as



**Fig. 4.** Microstructure of DLC films deposited on ACM using single synthesis protocols: a) film P ( $\Delta T = 101^\circ\text{C}$ ); b) film Z ( $\Delta T = 0$ ); c) film N ( $\Delta T = -94^\circ\text{C}$ ); d) film N2 ( $\Delta T = -68^\circ\text{C}$ ). Top: lower magnification (scale bars  $500 \mu\text{m}$ ); down: higher magnification (scale bars  $50 \mu\text{m}$ ).





**Fig. 5.** XSEM micrographs of DLC films deposited on ACM using single protocols with extreme values of  $\Delta T$ : a) film P ( $\Delta T = 101$  °C); b) film Z ( $\Delta T = 0$ ); c) film N ( $\Delta T = -94$  °C). Top: lower magnification (scale bars 5  $\mu\text{m}$ ). Down: higher magnification (scale bars 1  $\mu\text{m}$ ).

the temperature is getting closer to the equilibrium, while the growth rate of the film is constant during the whole deposition. Therefore, there is a moment where a continuous film is grown (sketched in the second row). From this point, a further temperature increase causes the formation of cracks in the film. At the end of the deposition, the cracks appear closed (as seen in Fig. 5c), since the substrate shrinks back when the process is finished and the temperature lowers from the final deposition temperature (around 145 °C) to room temperature. In contrast, in the case of the film N (see Fig. 6b), the rubber shrinks from the beginning of deposition, due to the continuous decrease of temperature. As a response to the compressive stress, a network of wrinkles forms in the DLC film that has a much smaller thermal expansion coefficient than the rubber. The difference of patch size observed in the films P and N, despite a close  $|\Delta T|$  can be explained using this scheme. In the case of  $\Delta T < 0$ , the compressive stress is acting from the beginning of the deposition and favors the formation of a continuous film, even considering a columnar growth. In the case of  $\Delta T > 0$ , the tensile stress hinders the formation of a continuous film, which can be formed only when the expansion of rubber substrate slows down. Thus, the formation of crack network is delayed.

As described above, the difference among the preparation protocols of the films was not only the sign of  $\Delta T$ , but also the different

bias voltages during growth (cf. Table 1). Thus, different deposition speeds and even different film properties may be expected, which could account for the different microstructures observed. Therefore, in order to validate the growth scheme presented in Fig. 6, two specific films were prepared in such a way that the same deposition voltage (462 V) was used, and also the same value of  $|\Delta T| = 46$  °C was obtained (cf. Fig. 7a). Fig. 7b and c show the microstructures of both films. In both cases, the patch sizes are much larger than the observed in previous cases, since the values of  $|\Delta T|$  are smaller. It can be seen that the patch size of film grown at  $\Delta T < 0$  (128  $\mu\text{m}$ ) is lower than in the case of the film prepared at  $\Delta T > 0$  (164  $\mu\text{m}$ ). Therefore, the growth schematics are confirmed.

The microstructures of the films prepared using double protocols are depicted in Fig. 8. Film NP shows smooth wrinkles, whereas in the case of film PN more cracking can be observed on the film. In both cases, the microstructures resemble that of films N and P. In fact, the double protocols used to prepare films NP and PN were the same as the films N and P, except an extra variation of temperature introduced at the final stage of the deposition (cf. Fig. 3). In addition, it can be seen that the patch size is intermediate between those of the corresponding films prepared using single protocols. In particular, it seems that the first temperature variation dominates the growth mode of the films, since film NP shows a patch size (80  $\mu\text{m}$ ) closer the one of film N, while film PN shows a patch size (100  $\mu\text{m}$ ) closer to film P. Therefore, it can be concluded that the microstructure is controlled by the process applied at the beginning of film growth.

Fig. 9 shows the CoF of different films. It can be seen that the values of CoF are low in comparison with the unprotected rubber (CoF  $\sim 0.7$ ). None of the curves achieve a steady state, and a continuous growth is seen instead. This is caused by the viscoelastic characteristics of rubber, which lead to a variable size and shape of the contact area between the counterpart ball and the film. In addition, it can be observed that the film Z (prepared at  $\Delta T = 0$  and not showing any crack pattern), shows the largest value of CoF around 0.26. In contrast, the other tile-like films exhibit a smaller CoF around 0.22. Nevertheless, slight differences can be distinguished within this group; the lowest and highest values correspond to films N and P, respectively, which are the films prepared using single protocols. Both the films prepared using double protocols show intermediate values. In fact, it seems that the CoF is correlated to the patch size such that lower the patch size, lower the CoF. This could be attributed to an improved

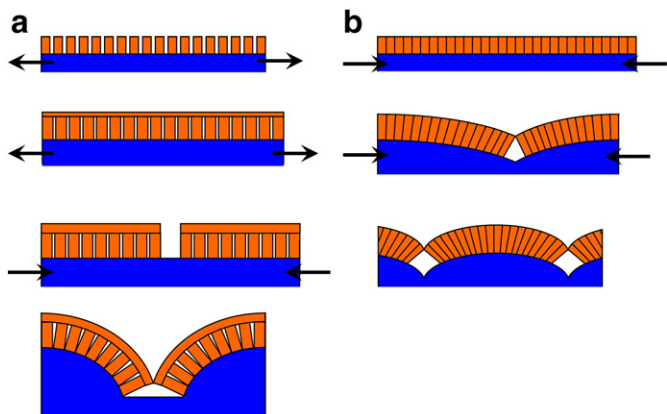


**Fig. 6.** Scheme (not to scale) of DLC film growth: (a) protocol with  $\Delta T > 0$  and (b) protocol with  $\Delta T < 0$ . The arrows indicate the direction of the stress.

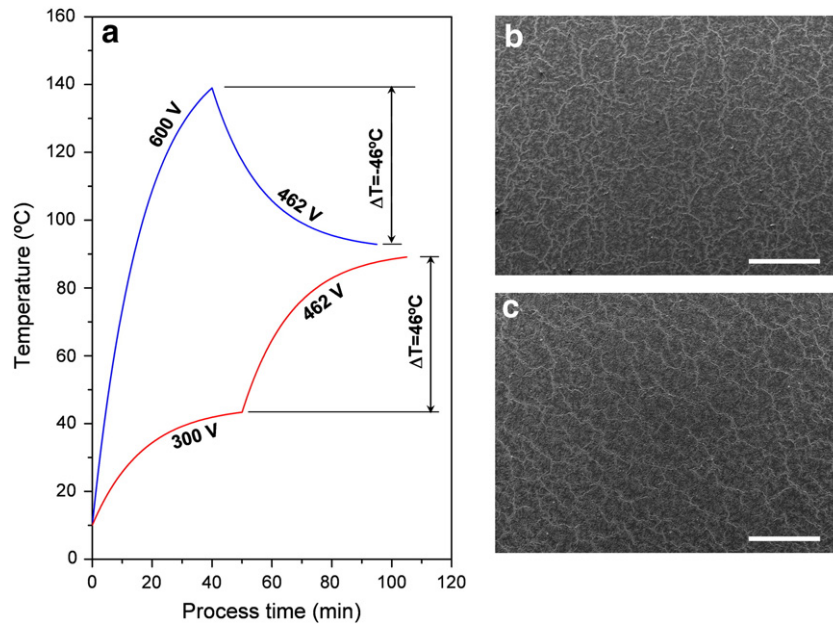


**Fig. 7.** Deposition of DLC films using the same bias voltage (462 V) and same  $|\Delta T| = 46^\circ\text{C}$ : a) deposition protocols, b) microstructure of film prepared at  $\Delta T = -46^\circ\text{C}$ , c) microstructure of film prepared at  $\Delta T = 46^\circ\text{C}$ . Scale bars: 500  $\mu\text{m}$ .

flexibility of the film as a result of the reduction of the patch size [5]. Finally, it is worth mentioning that, at the beginning of the test, the frictional behavior of films prepared by double protocols is the same as that observed for the films with corresponding single protocols. This observation reinforces the idea that the films prepared by double protocols are more influenced by the first value of  $\Delta T$  used.

#### 4. Conclusions

DLC films deposited on ACM rubber by PACVD with tailored microstructure and frictional performance have been obtained. The temperature of the substrate during deposition can be controlled by fine tuning of bias voltage and deposition time. Therefore, DLC films with different patch sizes can be deposited by using a proper sequence of treatments at different bias voltages. Smaller patch sizes are obtained at larger variations of temperature, since larger deformations are produced in the film during growth. In addition, negative

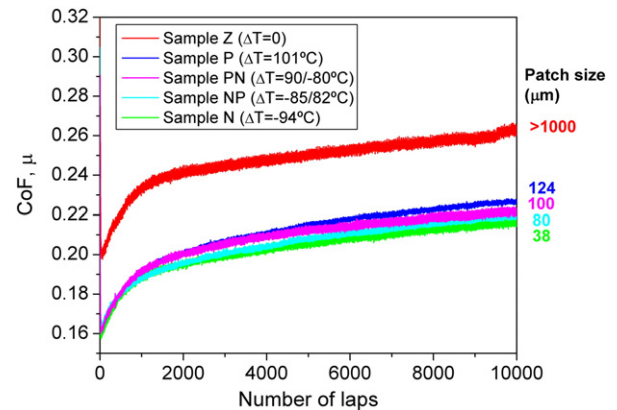


**Fig. 9.** CoF curves of DLC films with the patch sizes indicated on the right side.

variations of temperature leads to smaller patch sizes in comparison with positive variations of temperature, since tensile stress hinders the formation of a continuous film and thus delays film cracking. The coefficient of friction of DLC films coated ACM is much lower than that of unprotected rubber, with typical values around 0.22. Moreover, the coefficient of friction decreases upon decreasing patch size because of the enhanced flexibility of the film upon smaller patch size.

#### Acknowledgements

The financial support of Materials innovation institute (M2i), Delft, the Netherlands, under the project number MC7.06247 is gratefully acknowledged.

#### References

- [1] B.J. Hamrock, D. Dowson, Ball bearing lubrication, The Elastohydrodynamics of Elliptical Contacts, John Wiley & Sons Inc, 1981.
- [2] J. Robertson, Mater. Sci. Eng. R 37 (2002) 129.
- [3] T. Nakahigashi, Y. Tanaka, K. Miyake, H. Oohara, Tribol. Int. 37 (2004) 907.
- [4] X.L. Bui, Y.T. Pei, E.D.G. Mulder, J.T.M. De Hosson, Surf. Coat. Technol. 203 (2009) 1964.
- [5] Y.T. Pei, X.L. Bui, J.T.M. De Hosson, Scr. Mater. 63 (2010) 649.

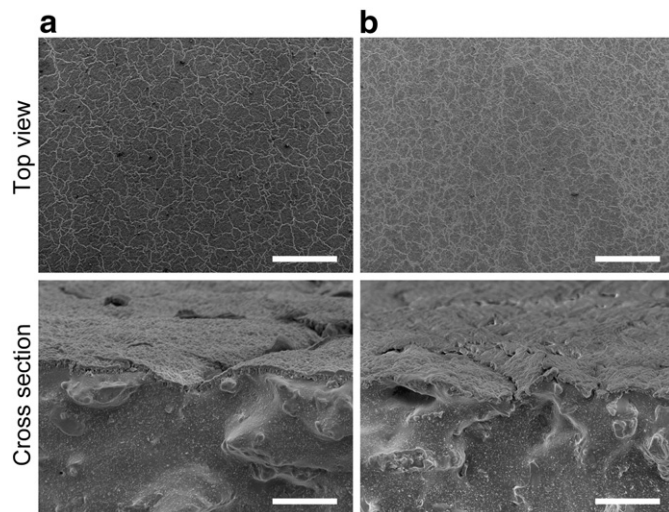


**Fig. 8.** Microstructure of DLC films deposited on ACM using mixed synthesis protocols: (a) film NP ( $\Delta T = -85/82^\circ\text{C}$ ) and (b) film PN ( $\Delta T = 90/-80^\circ\text{C}$ ). Top: top view at low magnification (scale bars 500  $\mu\text{m}$ ). Bottom: cross section view (scale bars 5  $\mu\text{m}$ ).